Radbound Repository

Radboud University Nijmegen

PDF hosted at the Radboud Repository of the Radboud University Nijmegen

The following full text is a publisher's version.

For additional information about this publication click this link.
http://hdl.handle.net/2066/92246

Please be advised that this information was generated on 2020-12-04 and may be subject to change.

PHYSICAL REVIEW B **83**, 045106 (2011)

# Quantum critical metamagnetism of $Sr_3Ru_2O_7$ under hydrostatic pressure

W. Wu,[1] A. McCollam,[2] S. A. Grigera,[3] R. S. Perry,[4] A. P. Mackenzie,[3,5] and S. R. Julian[1,5,*]
[1]*Department of Physics, University of Toronto, 60 St. George Street, Toronto, Ontario M5S 1A7, Canada*
[2]*Radbout University Nijmegen, High Field Laboratory, Faculty of Science, P.O. Box 9010, NL-6500 GL Nijmegen, The Netherlands*
[3]*Scottish Universities Physics Alliance, School of Physics and Astronomy, University of St. Andrews, North Haugh, St. Andrews KY16 9SS, United Kingdom*
[4]*Center for Science at Extreme Conditions, School of Physics, University of Edinburgh, Edinburgh, EH9 3JZ, Scotland*
[5]*Canadian Institute for Advanced Research, Quantum Materials Program, 180 Dundas St. W., Suite 1400, Toronto, Ontario M5G 1Z8, Canada*

(Received 27 September 2010; published 25 January 2011)

Using ac susceptibility, we have determined the pressure dependence of the metamagnetic critical endpoint temperature $T^*$ for a field applied in the *ab* plane in the itinerant metamagnet $Sr_3Ru_2O_7$. We find that $T^*$ falls monotonically to zero as pressure increases, producing a quantum critical endpoint (QCEP) at $P_c \sim 13.6 \pm 0.2$ kbar. New features are observed near the QCEP—the slope of $T^*$ versus pressure changes at ~12.8 kbar, and weak subsidiary maxima appear on either side of the main susceptibility peak at pressures near $P_c$—indicating that some new physics comes into play near the QCEP. Clear signatures of a nematic phase, however, that were seen in field-angle tuning of $T^*$ are not observed. As $T^*$ is suppressed by pressure, the metamagnetic peak in the susceptibility remains sharp as a function of an applied magnetic field. As a function of temperature, however, the peak becomes broad with only a very weak maximum, suggesting that, near the QCEP, the uniform magnetization density is not the order parameter for the metamagnetic transition.

DOI: 10.1103/PhysRevB.83.045106 PACS number(s): 75.30.Kz, 71.27.+a, 75.20.En

## I. INTRODUCTION

Quantum criticality continues to attract a lot of interest, much of it in connection with its role in generating exotic behavior of correlated electron systems. The original model of a quantum critical point involved a second-order phase transition being shifted to 0 K by some nonthermal tuning parameter such as pressure, chemical doping, or magnetic field.[1] The $T \rightarrow 0$ critical point, i.e., the quantum critical point (QCP), gives rise to nontrivial emergent excitations that control the physics over a significant portion of the phase diagram. In metals, electrons show non-Fermi liquid behavior in the quantum critical region, but also, near the QCP, electrons show a strong tendency to reorganize themselves into new stable phases such as exotic superconducting states.

Recently, a new kind of quantum critical point, associated with a first-order metamagnetic phase transition (MMT) in which no symmetry is broken, has been observed in $Sr_3Ru_2O_7$. Metamagnetism is empirically defined as a superlinear change of magnetization versus magnetic field in a narrow field range (a discontinuous jump in magnetization in the case of a first-order MMT). Quantum criticality is achieved by suppressing the endpoint of this first-order phase transition to absolute zero.[2] The term "quantum critical endpoint" (QCEP) is used to distinguish this from a QCP that involves symmetry breaking.

Figure 1 shows the suggested "generic" phase diagram of a metal on the border of ferromagnetism.[3–5] It has been applied, for example, to $CoS_2$,[6] MnSi,[3] $CeRu_2Si_2$,[7] and $UGe_2$.[8]

In this model, a second-order phase transition to a spontaneously ordered ferromagnetic state occurs at $T_c$ at $H = 0$. $T_c$ is then suppressed by a tuning parameter such as hydrostatic pressure, but as $T_c$ falls, it encounters a tricritical point (TCP) at which the second-order transition becomes first order. At the TCP, two metamagnetic "wings" emerge (at positive and negative magnetic field), representing surfaces at which there is a first-order metamagnetic jump in the magnetization as a function of applied magnetic field $H$. The top of the wings is delimited by a line of critical points $T^*(H,P)$, which separates the first-order jump from a continuous superlinear crossover behavior in the $M$ versus $H$ curve. This is illustrated in Fig. 1(i): As $H$ is increased along an isotherm with $T < T^*$, represented by the dashed line labeled $c$, the magnetization jumps discontinuously when the line passes through the surface; alternatively, if $T > T^*$, as in line $a$, there is no discontinuity, only a crossover. At $T^*$ the magnetic susceptibility, $\chi = dM/dH$, should diverge. The point on the phase diagram at which $T^* \rightarrow 0$ K is the quantum critical endpoint.[2]

There is considerable interest in the behavior near the quantum critical endpoint in $Sr_3Ru_2O_7$.[9–11] At ambient pressure, for magnetic fields applied parallel to the *ab* plane so that the magnetic-field angle $\theta$ is equal to zero, $Sr_3Ru_2O_7$ is believed to lie on the generic phase diagram roughly where the dashed lines, labeled $a$, $b$, or $c$, are situated in Fig. 1. That is, the ground state of $Sr_3Ru_2O_7$ is paramagnetic, but it is very close to being ferromagnetic, as demonstrated by the fact that, while highly hydrostatic pressure drives $Sr_3Ru_2O_7$ *away* from ferromagnetism[12,13] and causes the MMT field to increase,[14] uniaxial stress applied in the $c$-axis direction[13,15] drives the system *to* ferromagnetism at very low uniaxial stresses of around 1 kbar. (Note that the first high-pressure study of $Sr_3Ru_2O_7$ inadvertently had a large uniaxial stress component and produced ferromagnetism around 10 kbar.)[16] In an applied magnetic field, rotating the field away from the *ab* plane to the magnetically harder $c$ axis seems to be equivalent to tuning away from ferromagnetic order: $T^*$ falls, and a study of $T^*$ versus $\theta$ for "high-purity" single crystals (having residual resistivity $\rho_o \sim 2.4\ \mu\Omega$ cm) shows that the QCEP, $T^* \rightarrow 0$ K, occurs at about $\theta = 80°$.[17]

In even higher-purity samples, however, having $\rho_o < 0.5\ \mu\Omega$ cm and referred to in this paper as "ultrapure," $T^*$ does not go to zero as a function of $\theta$; rather it has a

©2011 American Physical Society

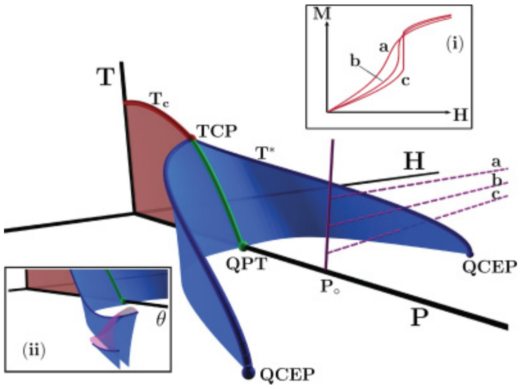

FIG. 1. (Color online) Main figure: Proposed generic phase diagram of a metal near the border of ferromagnetism.[3–5] As the ferromagnetic transition temperature $T_c$ is suppressed by a control parameter $P$, it changes from second to first order at a tricritical point (TCP). From the line of first-order transitions connecting TCP with the first-order quantum phase transition (QPT), two metamagnetic "wings" emerge (blue surfaces), corresponding to surfaces in $(T,P,H)$ space at which the magnetization jumps discontinuously [inset (i)]. The line of critical endpoints $T^*$ goes to 0 K at the quantum critical endpoint (QCEP). In ultrapure $Sr_3Ru_2O_7$, as $T^*$ is tuned by the angle of the magnetic field, the QCEP does not appear. Instead, a nematic phase is found, enclosed on the sides by two first-order metamagnetic jumps, and on top by a probable second-order phase boundary [inset (ii)].

minimum around $\theta \sim 60^\circ$ and then rises again accompanied by another, nearby, first-order jump at a slightly higher field. This is illustrated schematically in Fig. 1(ii). It has been shown that these two first-order transitions enclose a novel nematic phase [the region under the pink dome in Fig. 1(ii)] with strongly anisotropic transport properties that break the symmetry of the lattice.[9,10] The nature of the nematic phase is not well understood, but it has been speculated that the nematic phase maybe a result of a d-wave distortion of the Fermi surface arising from a Pomeranchuk instability.[9,18–20] Recently it was proposed that the nematic phase is a spatially modulated magnetic state analogous to a Fulde-Ferrell-Larkin-Ovchinnikov (LOFF) phase.[21,22]

Prior to $Sr_3Ru_2O_7$, MMTs had been reported in several other d- or f-electron metals such as $UPt_3$[23] and $URu_2Si_2$.[24] However, only in $Sr_3Ru_2O_7$ has it been possible to study the quantum critical endpoint, and these studies have been limited to field-angle tuning as we have described. Field-angle tuning has been proposed to play a role analogous to pressure, based on the assumption that the field angle suppresses the metamagnetism through angle-dependent magnetostriction.[17] In this sense, the phase diagram with the field-angle as a tuning parameter could have a close relation to the pressure-induced phase diagram obtained from Ginzburg-Landau treatments.[3,25] However, in changing the field angle the symmetry also changes, and nematic signatures are strongest when the symmetry is high, i.e., when the field is close to either the $c$ axis or the $ab$ plane.[10] A different explanation of the role of the field angle, suggested by Raghu *et al.*[19] and Berridge *et al.*,[22] is that the field angle moves the system through the phase diagram via orbital effects, i.e., by modification of the band structure through the spin-orbit and orbital-Zeeman coupling.[19]

This change of symmetry and orbital coupling as the direction of the field is changed in field-angle tuning complicates the interpretation of the results. If the MMT were tuned with pressure, then the symmetry and angle-dependent orbital coupling would not change, and this provides strong motivation for exploring the metamagnetic quantum criticality of $Sr_3Ru_2O_7$ under hydrostatic pressure. An intriguing question is whether the new nematic phase appears with pressure tuning.

In this paper we report an investigation, using ac susceptibility under hydrostatic pressure, of the metamagnetic quantum criticality of ultrapure crystals of $Sr_3Ru_2O_7$ for fields applied in the $ab$ plane. Compared to $H \parallel c$ where the nematic phase has already been observed, using $H \parallel (ab)$ has the disadvantage that the magnetic field breaks the in-plane symmetry; however, we wished, in this first study at least, to follow the evolution of the critical endpoint as a function of pressure, and this is not possible for $H \parallel c$ because the field angle has already tuned the system to the quantum critical region even at zero pressure. We note that weak signatures of nematicity have been reported for $H \parallel (ab)$, although not at the primary MMT.[26] We found that $T^*$ decreases monotonically with increasing pressure, going rather suddenly to zero above 12.8 kbar. The QCEP occurs at $P_c \sim 13.6 \pm 0.2$ kbar. We also observed that the divergence of the susceptibility at $T^*$, illustrated by the slope of curve (b) in Fig. 1(i), weakens dramatically as $P_c$ is approached, suggesting that the naive picture of metamagnetism as field-induced ferromagnetism may not apply to $Sr_3Ru_2O_7$ near the QCEP; rather it may arise from the suppression of antiferromagnetic correlations or a change in some higher-order correlation function of the electron system.

## II. EXPERIMENT

Hydrostatic pressure was applied using a BeCu clamp cell. To achieve a highly homogeneous pressure, Daphne oil 7373 was used as the transmitting medium. The pressure at low temperatures was determined from the known pressure dependence of the superconducting transition temperature of tin. The ac susceptibility was measured using a set of detection coils and a drive coil. The detection coil set comprises three coils, with the central coil connected antiparallel to the two end coils. The drive coil is concentrically wound around the three pick-up coils. This configuration significantly reduces background pick-up from the feedthrough that carries the wires into the high-pressure region, allowing us to see the metamagnetic peak more clearly. A low-frequency excitation field of 14 Hz, generated by the ac current in the drive coil, was employed to reduce finite-frequency effects.[27] At 13.4 kbar, 83 Hz was also used to test for frequency dependence. A sample with approximate dimensions ($0.7 \times 0.7 \times 1.7$ mm$^3$) was placed in the central pick-up coil and thermally grounded to the mixing chamber through silver and copper wires. The response of the sample was detected by a lock-in amplifier, preceded by a low-temperature transformer with a turns ratio of $\sim$100 and a $\times$1000 low-noise preamplifier. The sample used here was cut from an ultrapure single crystal of $Sr_3Ru_2O_7$ grown at St. Andrews University, UK. The residual resistivity was measured to be $\rho_\circ < 0.5$ $\mu\Omega$ cm.

For all the ac susceptibility measurements, the samples were cooled in zero field, and the dc field was applied in the $ab$

plane, i.e., parallel to the ac field. The sweep rate of the dc field was 0.02 T/min, the fastest rate for which there was no sign of heating in the lowest-temperature data. At pressures below 12.8 kbar we used only data from downsweeps, whereas at 12.8 kbar and above we averaged the results of up- and downsweeps. At the sweep rate of 0.02 T/min we did not resolve any hysteresis in the positions of the peaks between up- and downsweeps, beyond the lag that is expected from the time constants of our measurement system. (Unambiguous evidence for hysteresis is, however, supplied by the presence of a peak in the imaginary part of the susceptibility, which we describe below.) In averaging up- and downsweeps, as was done at 12.8 kbar and above, we first shifted the field axes by the tiny amount required to make positions of the peaks match.

In this investigation, we are only interested in the relative variation of the ac susceptibility due to the MMT ($\Delta\chi$), so a slowly varying background signal including the paramagnetic susceptibility of $Sr_3Ru_2O_7$ has been subtracted using a 5th-degree polynomial fit. The amplitude of the ac modulation field was approximately 0.1 G. The absolute ac susceptibility was left unresolved, and therefore arbitrary units (a.u.) are used in all the figures; however, the relative amplitude of the peaks at different pressures can be compared directly, as the same modulation amplitude and frequency, and the same electronics, were used throughout.

## III. RESULTS

Figure 2 shows the ac susceptibility of $Sr_3Ru_2O_7$, $\Delta\chi$, as a function of decreasing dc field under a hydrostatic pressure of 0.59 kbar. The real part of the ac susceptibility, $\Delta\chi'$, exhibits a pronounced peak, numbered 1 in Fig. 2, across the MMT at a field $H_M \approx 5.3$ T, and two minor peaks, numbered 2 and 3, at higher fields, $H \approx 6.06$ T and $H \approx 6.6$ T. These features are believed to reflect sharp peaks in the density of states, such as would arise for example from a van Hove singularity,[9,18] but a detailed connection with the rather complex electronic structure of $Sr_3Ru_2O_7$[28] has not yet been possible. Peak 2 at $H \approx 6.06$ T evolves into a double feature with decreasing temperature, reminiscent of the static differential susceptibility reported for this peak in Ref. 26. As can be seen from Fig. 2(c), using data that we will describe, we followed peaks 1 and 2 up to 18 kbar, finding that both peaks shift to a higher field roughly linearly with increasing pressure. Peak 1 increases with pressure at a rate of 0.3 T/kbar up to 18.2 kbar, while $H_c$ for peak 2 rises somewhat faster: the separation between peaks 1 and 2 expands from 0.79 T at 0.59 kbar to 2.63 T at 18.2 kbar. The size of peak 2 depends more weakly on pressure and temperature than that of peaks 1 and 3, and in fact peak 3 disappears quickly with rising temperature and pressure. Within the temperature and pressure range studied we were unable to resolve any imaginary part of the susceptibility for either peak 2 or peak 3.

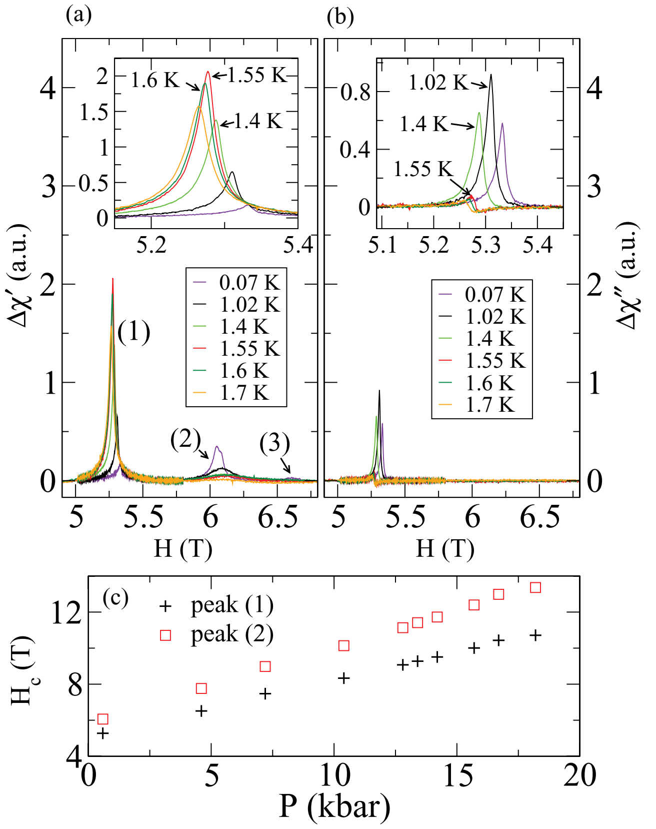

FIG. 2. (Color online) Real (a) and imaginary (b) parts of the ac magnetic susceptibility of $Sr_3Ru_2O_7$ at 0.59 kbar as the in-plane dc field is swept through the MMT. The data are labeled as $\Delta\chi'$ and $\Delta\chi''$, respectively; a slowly varying background has been subtracted. Although we use arbitrary units, the same coil and sample are used in all measurements so relative amplitudes at different pressures can be compared. Three successive peaks are observed in the susceptibility, numbered 1, 2, and 3 in (a). The inset in each panel shows an expanded plot around peak (1), which is the focus of this paper. For peak 1, with decreasing temperature from 1.7 K, $\Delta\chi'_{\rm max}$ initially grows, reaches a maximum at $T^* = 1.55$ K, and then decreases as the temperature is further reduced. (b) The peak in $\Delta\chi''$ starts to appear only below $T^* = 1.55$ K and then increases rapidly in amplitude as the temperature is reduced. No signal in $\Delta\chi''$ is observed at the positions of peaks 2 or 3. The small step in $\Delta\chi''$ at temperatures above 1.55 K may be the result of changing eddy currents in the sample. (c) Pressure dependence of the critical metamagnetic field $H_c$ at $T^*$, as a function of pressure for peaks 1 and 2. For pressures above 13.4 kbar, $H_c$ at ∼ 0.07 K is used.

For peak 1, Fig. 2(a) shows that the peak in $\Delta\chi'$ reaches its maximum at 1.55 K, while Fig. 2(b) shows that the corresponding imaginary part $\Delta\chi''$ of the ac susceptibility starts growing only below 1.55 K. This behavior arises from a first-order MMT terminating in a critical point at a temperature $T^* \sim 1.55$ K:[17] above $T^*$, the $M$ versus $H$ curve is a crossover that sharpens as $T \to T^*$; below $T^*$, the dynamical response becomes sensitive to the physics of a first-order MMT, such as domain wall movement, so that the real part of the ac susceptibility decreases while the imaginary part grows. It is also observed that the metamagnetic critical field has a weak temperature dependence, decreasing by 0.074 T from 0.1 to 1.8 K.

Data such as that shown in Fig. 2 has been collected at 0.59, 4.6, 7.2, 10.4, 12.8, 13.4, 14.2, 15.7, 16.7, and 18.2 kbar. As pressure increases from 0.59 kbar, the critical temperature $T^*$ decreases, while $H_M$ moves toward a higher field. As shown in Fig. 3(a), by 12.8 kbar, $T^*$ has fallen to $0.375 \pm 0.025$ K. At this pressure new structure has appeared both above and below the main peak in $\Delta\chi'$. To the right there is a pronounced bump, or secondary maximum, in $\Delta\chi'$, indicated by the red

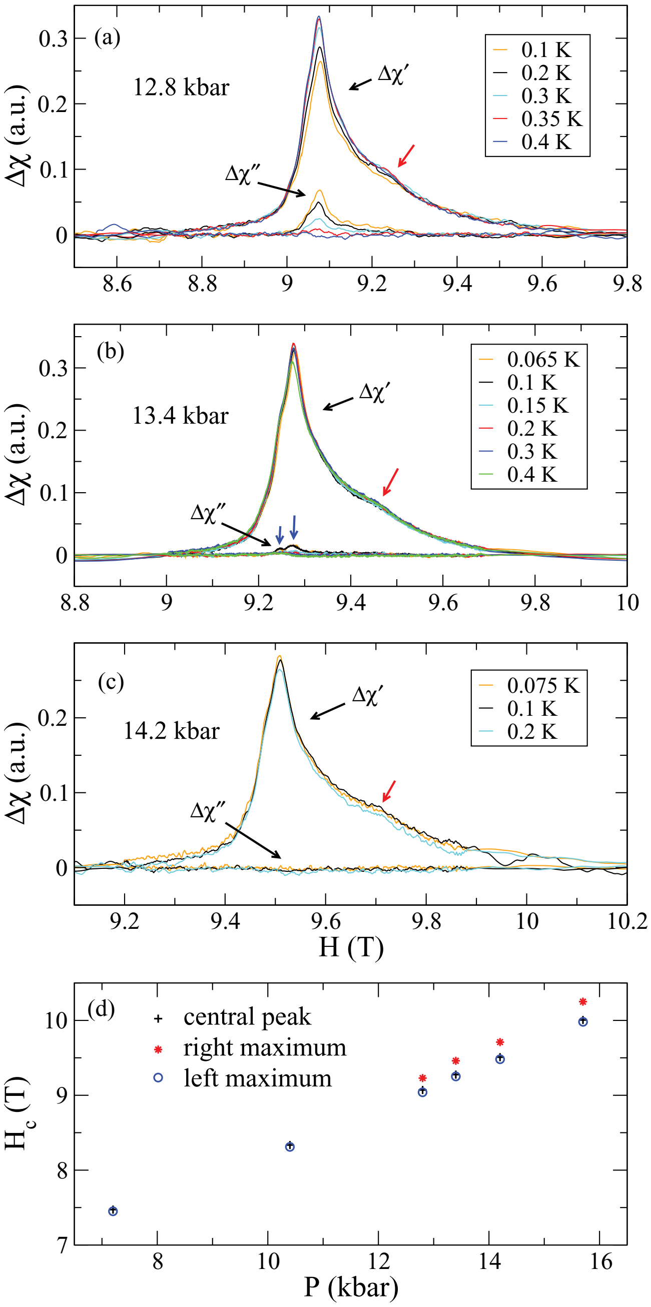

FIG. 3. (Color online) Temperature evolution of the ac susceptibility across the MMT for 12.8 kbar (a), 13.4 kbar (b), and 14.2 kbar (c). A secondary maximum to the right of the central peak of $\Delta\chi'$ is marked by the red arrow. $\Delta\chi''$ shows a clear peak below 0.3 K at 12.8 kbar, a much weaker peak below 0.15 K at 13.4 kbar, and no peak down to 0.07 K at 14.2 kbar. At 13.4 kbar, a double-peak feature can be seen in $\Delta\chi''$. Note that the scales on both the vertical and horizontal axes are different for the three graphs (a), (b), and (c). (d) Critical metamagnetic field $H_c$ at $T^*$ as a function of pressure for peak 1 and of the two secondary maxima in $\Delta\chi'$ at $T^*$. For pressures above 13.4 kbar, $H_c$ at ~0.07 K is used, as in Fig. 2(c).

arrow in Fig. 3(a). $\Delta\chi''$ extends asymmetrically out to this secondary maximum. Similarly, just below the main peak a weak secondary maximum is seen in both $\Delta\chi'$ and $\Delta\chi''$.

At 13.4 kbar, $T^* \sim 0.15$ K, and the secondary maxima become more clear in comparison with 12.8 kbar.

The dissipation signal corresponding to the central peak in $\Delta\chi'$ diminishes but is still visible; by 13.4 kbar, it has evolved into two distinct peaks [see the blue arrows in Fig. 3(b)]. The left peak in $\Delta\chi''$ matches the secondary maximum just below the main peak in $\Delta\chi'$; however, $\Delta\chi''$ is zero, within our resolution, at the secondary maximum on the right.

At 14.2 kbar [see Fig. 3(c)], $T^*$ has fallen below 0.07 K, the lowest temperature reached in these measurements. $\Delta\chi''$ remains flat down to 0.07 K, showing that the peaks in $\Delta\chi'$ are crossovers. The secondary maxima to the right and left of the central maximum in $\Delta\chi'$ are still discernible at this pressure.

Figure 3(d) zooms in on the portion of Fig. 2(c) close to $P_c$, showing the shift with pressure of the central peak and the two secondary maxima. It can be seen that the features all shift together, and there is no visible change in slope at $P_c$.

The $(T^*,P,H)$ phase diagram is given in Fig. 4. This represents our measurement of the tip of a metamagnetic wing that is shown schematically in Fig. 1. The critical temperature $T^*$ falls uniformly from ~1.55 K at ~0.59 kbar to ~0.375 K at ~12.8 kbar; then $T^*$ drops quickly to below 0.07 K, the lowest temperature reached in these measurements. In the inset, the error bars at pressures above 14.2 kbar extend from zero to ~0.07 K, but it is reasonable to assume that $T^*$ has fallen to zero at approximately 13.6 kbar, making this the quantum critical endpoint pressure, $P_c \sim 13.6 \pm 0.2$ kbar. Above $P_c$, the peak in $\Delta\chi''$ has disappeared, while the central peak in $\Delta\chi'$ persists. The secondary maximum above the main peak weakens as the pressure is further increased and disappears at ~16.7 kbar.

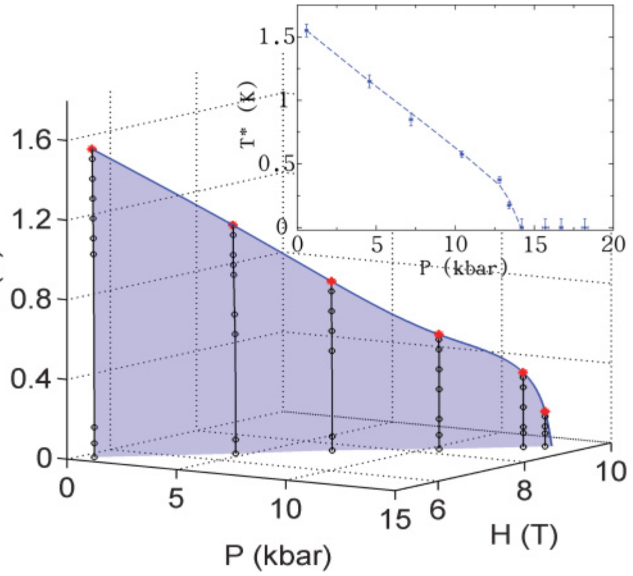

FIG. 4. (Color online) The phase diagram inferred from susceptibility measurements. The blue and black solid lines are splines of the measured critical endpoints $T^*$ (red) and the position of the MMT below $T^*$ as a function of temperature and field (black) at each pressure, respectively. (Inset) Projection of the line of critical endpoints in the $(P,T)$ plane. For pressures larger than 14.2 kbar, 0.07 K is taken as the error bar for the critical temperatures because that was the lowest temperature reached. The quantum critical endpoint is close to 13.6 kbar. The dashed line in the inset is a guide to the eye.

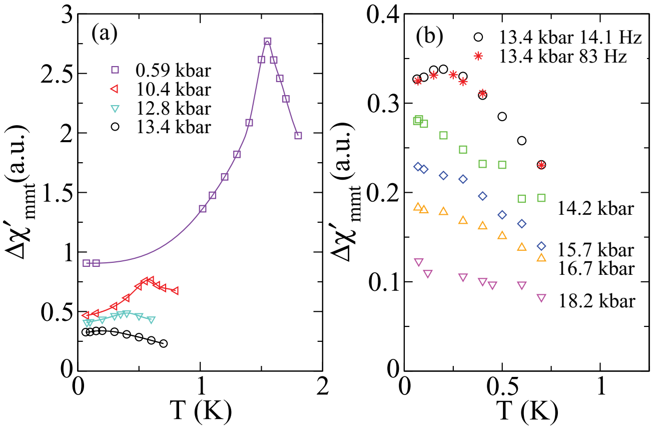

FIG. 5. (Color online) The magnitude of $\Delta\chi'$ at the MMT field, $\Delta\chi'_{\rm mmt}$, as a function of temperature for several pressures, showing the dramatic fall in $\Delta\chi'_{\rm mmt}$ as the quantum critical endpoint is approached. (a) Data below $P_c$; note that the data below 13.4 kbar have been offset to avoid overlap. (b) Expanded plot of the higher-pressure data; the datasets for 13.4 kbar show that frequency has little effect on the temperature dependence of $\Delta\chi'_{\rm mmt}$. Note that the gain settings for the two datasets at 13.4 kbar are different, so the 83 Hz curve has been rescaled by a multiplicative factor to agree with the 14.1 Hz curve at 0.75 K.

Figures 2 and 3 show $\Delta\chi'$ versus $H$ sweeps at constant temperatures. Comparing these figures, we observe the surprising result that although the metamagnetic peak has a strong temperature dependence near $T^*$ at low pressures (Fig. 2), for pressures near $P_c$ (Fig. 3) this has become very weak.

This is emphasized in Fig. 5, which plots the temperature dependence of the maximum in $\Delta\chi'$. Clearly the peak at $T^*$ collapses drastically with increasing pressure: As $P_c$ is approached, the maximum becomes much weaker, and near the quantum critical endpoint it has nearly disappeared. This phenomenon has little frequency dependence: Fig. 5(b) includes data for two different frequencies, 14.1 and 83 Hz, at 13.4 kbar, and the two datasets closely overlap.

## IV. DISCUSSION

We have found that, for $H \parallel ab$, application of hydrostatic pressure produces a quantum critical endpoint at $13.6 \pm 0.2$ kbar in $Sr_3Ru_2O_7$. This opens new avenues for studying quantum criticality and metamagnetism in this material.

As with field-angle tuning from the *ab* plane to the *c*-axis, hydrostatic pressure causes a monotonic increase in the MMT field $H_M$ and moves the system away from ferromagnetic order (see Fig. 1). However, the phase diagram produced by pressure tuning (see Fig. 4) looks very different from that produced by field-angle tuning for the same ultrapure-quality crystals.[9,10] In the latter case, as the system is tuned away from ferromagnetism, the QCEP is avoided due to the appearance of the nematic phase bounded by first-order metamagnetic jumps, so $T^*$ never goes to zero; rather, it has a minimum at $\theta \sim 60^\circ$ and then rises again as the nematic phase emerges. With pressure, in contrast, $T^*$ goes to zero, apparently smoothly.

However, despite the similarity of Fig. 4 to the tip of the metamagnetic wing in the generic phase diagram (Fig. 1), the underlying physics seems to be quite different. According to the generic model of quantum critical metamagnetism,[29] the susceptibility should be divergent at $T^*$, but Fig. 5 shows that the maximum in $\Delta\chi'_{\rm mmt}$ at $T^*$ drops quickly with increasing pressure, even at pressures well below $P_c$. This would mean that as the quantum critical endpoint is approached, the metamagnetic quantum criticality is not dominated by long-wavelength magnetic fluctuations as would be naively expected if the uniform magnetization density is the order parameter for the MMT. In other words, the MMT near the QCEP does not seem to correspond to field-induced ferromagnetism; rather, the important fluctuations near the QCEP may be at short wavelength, or they may not be magnetic at all. A possible scenario is that the first-order jump in the magnetization near the QCEP could arise from the sudden disappearance of antiferromagnetic correlations, rather than entry into a field-induced ferromagnetic state. This may be consistent with the suggestion that the nematic phase is a spatially modulated magnetic state as predicted in Refs. 21 and 22.

In high-purity crystals, field-angle tuned measurements also observed that $\Delta\chi'_{\rm mmt}(T^*)$ drops dramatically as the QCEP is approached.[17] It was suggested that the expected divergence of $\chi$ at $T^*$ was being suppressed by impurity-enhanced critical slowing down, so that the finite frequency (~80 Hz) used in these ac susceptibility measurements is not a good approximation to the zero-frequency limit, and therefore the genuine divergence in the long-wavelength limit was not unveiled.[17] However, because we used ultrapure crystals, with five-times lower residual resistivity and a significantly lower measurement frequency (~14 Hz), we feel that it is unlikely that the susceptibility would diverge, even if it were measured at zero frequency. This is further supported by our observation that the frequency dependence of the relative variation of $\Delta\chi'_{\rm mmt}$ is extremely weak: at 13.4 kbar, $\Delta\chi'_{\rm mmt}$ versus $T$ shows almost no difference between 83 and 14 Hz [see Fig. 5(b)].

Note that pressure inhomogeneity also cannot account for the suppression of the peak in $\chi$ at $T^*$. In our measurements we have some indication of pressure inhomogeneity from the width of the superconducting transition of the tin wire used as a pressure gauge, and from the width of the peaks in $\chi$. From these we know that the pressure inhomogeneity is very small, as expected for the pressure medium, Daphne oil 7373, at this pressure.[30] Moreover, at a given pressure, inhomogeneity in the pressure would broaden the peaks in $\chi$ at all temperatures, so we would still expect to see some enhancement of $\Delta\chi'_{\rm mmt}$ at $T^*$, if such a maximum in $\Delta\chi'_{\rm mmt}$ were present with homogeneous pressure, even if the divergence is partially suppressed; what we actually observe is that the maximum disappears almost completely as the QCEP is approached.

The temperature dependence of $H_M$ at different fixed pressures, as shown in Fig. 6, could also be interpreted as evidence of the importance of quantum fluctuations at finite $q$, or higher-order correlations in the electron system. The decrease of $H_M$ with increasing temperature, which is at first sight surprising within a simple picture of metamagnetism, has in the past been explained as arising from a growth of quantum fluctuations at long wavelength with decreasing temperature, although Berridge has recently shown that similar curves are generated within a Stoner theory.[29,31] In either scenario, however, one might expect the curvature of $H_M$ to change at

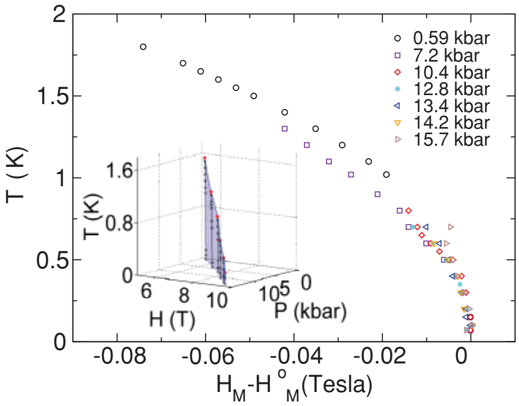

FIG. 6. (Color online) Temperature dependence of the MMT field $H_M$ for each pressure as viewed in the $(H,T)$ plane, relative to the 70 mK value $H_M^\circ$ at each pressure. (Inset) $H_M$ viewed in the $(P,H,T)$ space without offset to show that the curvature of the metamagnetic "wing" is rather small, although on a fine scale, as shown in the main figure, it is clearly visible.

$P_c$, whereas we find that the curvature of $H_M$ at $P_c$ is the same as at higher and lower pressures far from $P_c$.

Finally, our argument that the quantum critical fluctuations at the pressure-tuned QCEP are not ferromagnetic in nature is supported by other measurements at the field-angle tuned QCEP. Ambient-pressure neutron and NMR studies[32–34] show that antiferromagnetic fluctuations prevail over ferromagnetic at low temperatures (<20 K). In particular, inelastic neutron measurements reported by Ramos *et al.* show that, for $H \parallel c$, antiferromagnetic fluctuations are present in a wide field range (4–13 T) and become soft at the metamagnetic field.[32] The NMR study reported by Kitagawa *et al.* further points out that the quantum critical fluctuations at the quantum critical point of $Sr_3Ru_2O_7$ are antiferromagnetic.[34] The finite-$q$ magnetic fluctuations may be associated with the spatially modulated magnetic phase, i.e., the LOFF nematic phase, which is suggested to exist near the QCEP by Berridge *et al.*[21,22] The short-range correlations of the LOFF phase may be present outside of this phase and gain strength as the QCEP is approached;[19] this scenario may explain the disappearance of the sharpness of the peak in $\Delta\chi'_{\mathrm{mmt}}$ versus $T$ with increasing pressure.

Although pressure tuning for $H \parallel ab$ causes $T^*$ to go smoothly to 0 K, we do see different behavior emerging near the QCEP. First, there is a change of the slope $dT^*/dP$ at ~12.8 kbar (Fig. 4), indicating a change in the underlying physics. Second, there is the secondary maximum that appears on the right of the main peak in $\Delta\chi'$ (Fig. 3). This is present only in the region 12.8 to 16.7 kbar, that is, only near $P_c$, and is reminiscent of the double transition that encloses the nematic phase in the field-tuning measurements. We do not, however, observe a corresponding peak in $\Delta\chi''$ at this secondary maximum. Third, there is a secondary maximum in $\Delta\chi'$ just below the main peak that may correspond to a weakly split structure in $\Delta\chi''$ that starts from ~7 kbar and becomes clear at 13.4 kbar (Fig. 3). This is a very weak splitting, which we could resolve only by averaging many repeated runs, and the field interval is much smaller than is seen for the field-tuned nematic phase: ~0.027 T as opposed to ~0.25 T.

It should be noted that it may be possible to have the nematic phase without the bounding first-order transitions: The top of the nematic "dome" is defined by a second-order transition [Fig. 1(ii)]. Perhaps, under some conditions, only the top of the dome exists. In fact, because the field is being applied in the *ab* plane so that the in-plane symmetry is already broken, there may be no need for even a second-order phase transition, and it may be possible to enter the nematic state via a crossover.

At this stage, evidence for the nematic phase is not conclusive, and it will be important to carry out magnetotransport studies near $P_c$, as peaks in $\rho(B)$ at low temperature provide definitive evidence for the nematic phase.[9]

The only previous hydrostatic pressure study of the magnetoresistance of $Sr_3Ru_2O_7$ with $H \parallel ab$ was carried out on a high-purity sample at $T = 2.5$ K in the pressure range 0 to $\sim 10$ kbar.[14] This study showed a broad magnetoresistance peak around the MMT moving to a higher field with increasing pressure at a rate consistent with our observations; however, because the magnetoresistance was measured at a temperature well above $T^*$, and pressures well below $P_c = 13.6$, and on a sample that is not believed to be pure enough to exhibit the nematic phase, no conclusion can be drawn about the existence of the nematic phase from this work.

Finally, we address the issue of magnetovolume effects, which are known to play an important role in metamagnetism.[35] For instance, in $CeRu_2Si_2$ magnetovolume effects provide positive feedback to drastically sharpen what would be a broad crossover under constant volume.[7,35] In our measurements, the freezing of the pressure medium (Daphne oil 7373) at low temperatures (~200 K) may suppress positive magnetoelastic feedback in $Sr_3Ru_2O_7$, a system with a strong magnetoelastic coupling (the magnetic Grüneisen parameter $\Gamma_H > 100$).[36] This may broaden the peak in $\Delta\chi'$, connecting the secondary maxima and the central peak to produce weak "shoulders" rather than distinct separate peaks. We point out that some features observed around $P_c$ disappear at higher pressures, for instance, the secondary maximum to the right of the main peak in $\Delta\chi'$, so they are unlikely to be caused by pressure inhomogeneity in the transmitting medium.

## V. SUMMARY

In $Sr_3Ru_2O_7$, it has been previously established that a QCEP can be produced by tuning the magnetic field angle from the *ab* plane toward the *c* axis at ambient pressure, and that in an ultrapure sample this QCEP is avoided by the appearance of a nematic phase bounded by two first-order MMTs. In this work, we have used ac susceptibility measurements to show that, for $H \parallel ab$, hydrostatic pressure can also produce a QCEP in an ultrapure sample. We see that the critical endpoint temperature of the first-order MMT, $T^*$, falls monotonically as a function of pressure, going to zero rather suddenly above 12.8 kbar; the QCEP exists at $P_c = 13.6 \pm 0.2$ kbar. The signature of the nematic phase observed in field-angle tuning (two clearly resolved MMTs at the phase boundaries) is absent. We also observe that with increasing pressure the divergence of the susceptibility at the critical point diminishes quickly, suggesting that short-wavelength fluctuations may dominate the MMT as the QCEP is approached.

[*] sjulian@physics.utoronto.ca

[1] J. A. Hertz, Phys. Rev. B **14**, 1165 (1976).

[2] S. A. Grigera *et al.*, Science **294**, 329 (2001).

[3] C. Pfleiderer, S. R. Julian, and G. G. Lonzarich, Nature (London) **414**, 427 (2001).

[4] R. B. Griffiths, Physica **33**, 689 (1967).

[5] D. Belitz and T. R. Kirkpatrick, Phys. Rev. Lett. **89**, 247202 (2002).

[6] T. Goto, K. Fukamichi, and H. Yamada, Physica B **300**, 167 (2001).

[7] J. Flouquet, S. Kambe, L. P. Regnault, P. Haen, J. P. Brison, F. Lapierre, and P. Lejay, Physica B **215**, 77 (1995).

[8] V. Taufour, D. Aoki, G. Knebel, and J. Flouquet, Phys. Rev. Lett. **105**, 217201 (2010).

[9] S. A. Grigera *et al.*, Science **306**, 1154 (2004).

[10] R. A. Borzi, S. A. Grigera, J. Farrell, S. J. S. Lister, S. L. Lee, D. A. Tennaut, Y. Maeno, and A. P. Mackenzie, Science **315**, 214 (2007).

[11] A. W. Rost, R. S. Perry, J. F. Mercure, A. P. Mackenzie, and S. A. Grigera, Science **325**, 1360 (2009).

[12] Y. V. Sushko, B. DeHarak, G. Cao, G. Shaw, D. K. Powell, and J. W. Brill, Solid State Commun. **130**, 341 (2004).

[13] S. I. Ikeda, N. Shirakawa, S. Koiwai, A. Uchida, M. Kosaka, and Y. Uwatoko, Physica C **364–365**, 376 (2001).

[14] M. Chiao, C. Pfleiderer, S. R. Julian, G. G. Lonzarich, R. S. Perry, A. P. Mackenzie, and Y. Maeno, Physica B **312–313**, 698 (2002).

[15] S. I. Ikeda, N. Shirakawa, T. Yanagisawa, Y. Yoshida, S. Koikegami, S. Koike, M. Kosaka, and Y. Uwatoko, J. Phys. Soc. Jpn. **73**, 1322 (2004).

[16] S. I. Ikeda, Y. Maeno, S. Nakatsuji, M. Kosaka, and Y. Uwatoko, Phys. Rev. B **62**, R6089 (2000).

[17] S. A. Grigera, R. A. Borzi, A. P. Mackenzie, S. R. Julian, R. S. Perry, and Y. Maeno, Phys. Rev. B **67**, 214427 (2003).

[18] H. Y. Kee and Y. B. Kim, Phys. Rev. B **71**, 184402 (2005).

[19] S. Raghu, A. Paramekanti, E-.A. Kim, R. A. Borzi, S. A. Grigera, A. P. Mackenzie, and S. A. Kivelson, Phys. Rev. B **79**, 214402 (2009).

[20] W.-C. Lee and C. Wu, Phys. Rev. B **80**, 104438 (2009).

[21] A. M. Berridge, A. G. Green, S. A. Grigera, and B. D. Simons, Phys. Rev. Lett. **102**, 136404 (2009).

[22] A. M. Berridge, S. A. Grigera, B. D. Simons, and A. G. Green, Phys. Rev. B **81**, 054429 (2010).

[23] P. H. Frings, J. J. M. Franse, F. R. de Boer, and A. Menovsky, J. Magn. Magn. Mater. **31–34**, 240 (1983).

[24] A. de Visser, F. R. de Boer, A. A. Menovsky, and J. J. M. Franse, Solid State Commun. **64**, 527 (1987).

[25] S. A. Grigera, A. P. Mackenzie, A. J. Schofield, S. R. Julian, and G. G. Lonzarich, Int. J. Mod. Phys. B **16**, 3258 (2002).

[26] R. S. Perry, T. Tayama, K. Kitagawa, T. Sakakibara, K. Ishida, and Y. Maeno, J. Phys. Soc. Jpn. **74**, 1270 (2005).

[27] A. J. van Duyneveldt, J. Appl. Phys. **53**, 8006 (1982).

[28] J.-F. Mercure *et al.*, Phys. Rev. B **81**, 235103 (2010).

[29] A. J. Millis, A. J. Schofield, G. G. Lonzarich, and S. A. Grigera, Phys. Rev. Lett. **88**, 217204 (2002).

[30] K. Yokogawa, K. Murata, H. Yoshino, and S. Aoyama, Jpn. J. Appl. Phys. **46**, 3636 (2007).

[31] A. M. Berridge, e-print arXiv:1009.2777v1.

[32] S. Ramos *et al.*, Physica B **403**, 1270 (2008).

[33] L. Capogna, E. M. Forgan, S. M. Hayden, A. Wildes, J. A. Duffy, A. P. Mackenzie, R. S. Perry, S. Ikeda, Y. Maeno, and S. P. Brown, Phys. Rev. B **67**, 012504 (2003).

[34] K. Kitagawa, K. Ishida, R. S. Perry, T. Tayama, T. Sakakibara, and Y. Maeno, Phys. Rev. Lett. **95**, 127001 (2005).

[35] M. Chiao, C. Pfleiderer, R. Daou, A. McCollam, S. R. Julian, G. G. Lonzarich, R. S. Perry, A. P. Mackenzie, and Y. Maeno, e-print arXiv:cond-mat/0207697v1.

[36] P. Gegenwart, F. Weickert, R. S. Perry, and Y. Maeno, Physica B **378–380**, 117 (2006).